

Spring 2015

# Accretion Disk Spectra of Black Hole X-ray Binaries

Kristina Salgado  
Kristina.Salgado@Colorado.EDU

Follow this and additional works at: [http://scholar.colorado.edu/honr\\_theses](http://scholar.colorado.edu/honr_theses)

 Part of the [Other Astrophysics and Astronomy Commons](#), [Physical Processes Commons](#), and the [Stars, Interstellar Medium and the Galaxy Commons](#)

---

## Recommended Citation

Salgado, Kristina, "Accretion Disk Spectra of Black Hole X-ray Binaries" (2015). *Undergraduate Honors Theses*. Paper 933.

This Thesis is brought to you for free and open access by Honors Program at CU Scholar. It has been accepted for inclusion in Undergraduate Honors Theses by an authorized administrator of CU Scholar. For more information, please contact [cuscholaradmin@colorado.edu](mailto:cuscholaradmin@colorado.edu).

# **Accretion Disk Spectra from Black Hole X-ray Binaries**

**Kristina Salgado**

Department of Astrophysical and Planetary Sciences  
University of Colorado at Boulder

*April 2, 2015*

Senior honors thesis submitted in partial fulfillment for the  
Honors Astronomy Bachelor of Arts Degree

*Thesis Advisor*

Philip Armitage, Department of Astrophysical and Planetary Sciences

*Defense Committee*

Erica Ellingson, Department of Astrophysical and Planetary Sciences, Honors Council  
Representative

Lonni Pearce, Program for Writing and Rhetoric

## Abstract

Modeling black hole X-ray binaries is complex in nature due to the complicated physical processes occurring in the disk (i.e., scattering, absorption and emission, relativistic effects); however, the overall effect is a relatively minor shift of the emergent spectrum towards harder energies. A single parameter,  $f_{\text{col}}$  is generally used to phenomenologically capture the global effect on the observed spectrum. A  $\chi^2$  minimization routine was developed in order to fit three parameters to an accretion disk spectrum: a normalization constant, the maximum temperature of an accretion disk, and the spectral hardening factor  $f_{\text{col}}$  in an attempt to constrain  $f_{\text{col}}$ . However, a stronger parameter degeneracy than expected did not allow this to work. As a consequence,  $f_{\text{col}}$  was left as a constant, 1.0, and the algorithm successfully fit input disk spectra to my developed model by exploring combinations of  $N$  and  $T_{\text{max}}$ . In order to further the research, I will employ Markov Chain Monte Carlo methods to better explore the parameter space and learn how the vertical disk structure, specifically the reprocessing of energy in the disk's atmosphere, the corona, has an effect on the spectral hardening factor.

# 1 Introduction

Stellar mass black holes are formed when a massive star, much more massive than the Sun, explodes in a supernova — the star no longer undergoes fusion and cannot balance gravity with the usual radiation and gas pressure. Thus, the outer layers of the star are blown away and the star collapses in on itself to form an incredibly dense singularity. This object is so compact, that nothing —

including light, which is what astronomers observe — can escape its extreme gravity. Consequently, astronomers cannot observe a black hole directly and must resort to indirect means to study their exotic nature. Natural laboratories for studying black holes are systems called black hole X-ray binaries (hereafter, BHXRBS), of which only a few dozen are currently known in our Galaxy. As shown in the artist’s conception of Figure 1, a BHXRBS consists of a black hole, whose mass is roughly five to 15 times that of the Sun, in a binary orbit with a donor star.

The rarity<sup>1</sup> [13][23] of a BHXRBS can be attributed to the large number of improbable steps necessary for their formation. Of the two stars needed to create a BHXRBS, the donor star is considered the secondary star, since the much more massive primary star must evolve into a black hole via supernova. The donor star must first survive the blast from its partner, maintaining the binary system [16]. Following the supernova, the donor star rapidly evolves and a combination of gravitational and centrifugal forces create the Roche potential. Within this potential field, there is a critical figure-eight-shaped equipotential surface where both the star and compact object are enclosed, each within their own Roche lobe. The two are joined at the inner Lagrange point on the saddle between the two potential wells (see Figure 2).

The primary and most efficient method of accretion is via Roche-lobe overflow. This process occurs mainly in low-mass BHXRBS’s, where a main sequence star ( $\lesssim 1.4M_{\odot}$ ) exhausts its hydrogen fuel in the core, increasing its core temperature to begin helium fusion causing its outer hydrogen layers to also undergo fusion. Both of these processes increase the radiation pressure and the lighter outer layers are forced to expand to maintain the temperature gradient, allowing the star to fill its Roche lobe and

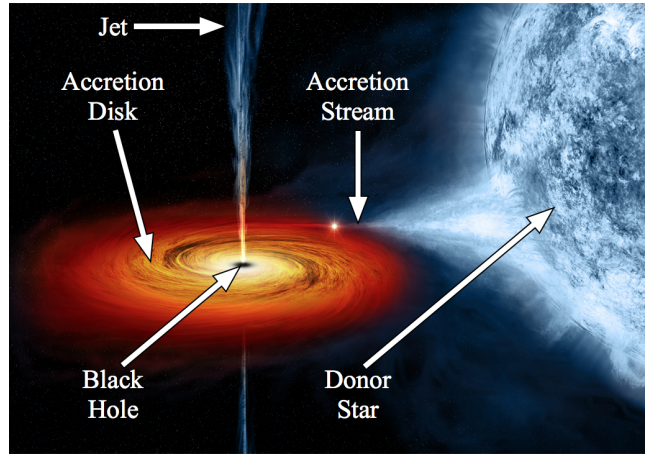


**Figure 1:** Anatomy of a black hole X-ray binary.

<sup>1</sup>Wijers (1996) and Romani (1998) estimate that there are  $\sim 2000$  BHXRBS in the Milky Way Galaxy.

begin mass transfer. The material passes through the inner Lagrange point via an accretion stream and the differential rotation profile of the disk forces the gas and dust to orbit the black hole before plunging in or being ejected into a jet. Because there is an instability producing an effective viscosity<sup>2</sup> within the disk, the material at smaller, faster orbits loses angular momentum to the larger, slower orbits, transferring angular momentum outward and spreading the material into an accretion disk. The other method of accretion is via stellar wind, but this only works for very strong winds from extremely massive stars.

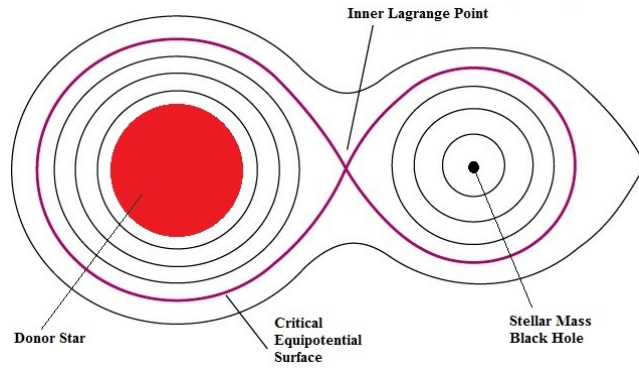


**Figure 2: Roche Geometry.**

As the gas in the accretion disk orbits faster and faster as it approaches the black hole, the gas heats up to temperatures exceeding 10 million degrees Kelvin. Therefore, the accretion disk glows as X-ray light and this radiation coming from the inner regions of the disk is what astronomers observe with space-borne X-ray telescopes. A major observational diagnostic for studying black holes

is the accretion disk spectrum, which is obtained by collecting the amount of X-ray radiation emitted by the disk across a range of discrete energy (or equivalently, frequency or wavelength) bins, usually with range of 0.1 – 10 keV. The *solid black line* in Figure 3 shows a representative case of a disk spectrum where the peak is determined by the temperature of the accretion disk. During the voyage from leaving the donor star to being lost forever inside the black hole, this accreting gas will release half of its total energy as radiation, while the other half is dumped into the black hole. However, many issues arise when observers receive the data from the telescopes. The best, most current telescopes that astronomers use can only detect energies as low as 0.2 keV, cutting off a large portion of the emergent spectrum of the BHXR. The other problem is the absorption of X-ray light by the interstellar medium. Imagine looking at a BHXR in one direction, then looking at another in a different direction. The column density of the interstellar medium between the telescope and the object observed varies throughout the Galaxy, making the absorption non-constant and difficult to account for [11]. Measurements of the column density are important for estimations of light absorption across all wavelengths and this is a current area of research in the astrophysical community.

In addition, a complication in observations stems from the structure of the accretion disk since it is

<sup>2</sup>Balbus & Hawley (1991) argue the magnetorotational instability (MRI), an instability involving magnetic fields and a differentially rotating disk of gas, creates turbulence in the disk and thus, an effective viscosity, not a viscosity in the usual molecular sense.

likely threaded by a magnetic field. While entire accretion disks cannot yet be simulated with sufficient resolution to capture all of the governing physics, the current state-of-the-art supercomputers permit local patches of the disk to be simulated at high resolution. Figure 4 shows a local simulation of an accretion disk and highlights the highly turbulent and strongly magnetized gas. These local simulations of accretion disks demonstrate that a significant amount of energy is lifted from the mid-plane of the accretion disk into the upper atmospheres of the disk, the corona, by magnetic buoyancy [20]. This energy is not necessarily released as radiation, as is generally assumed, but can instead go into heating the gas and accelerating particles [3]. Allowing these magnetic processes to influence energy transfer in the accretion disk can cause the emergent spectrum to change dramatically [10], as represented by the *red dotted line* in Figure 3.

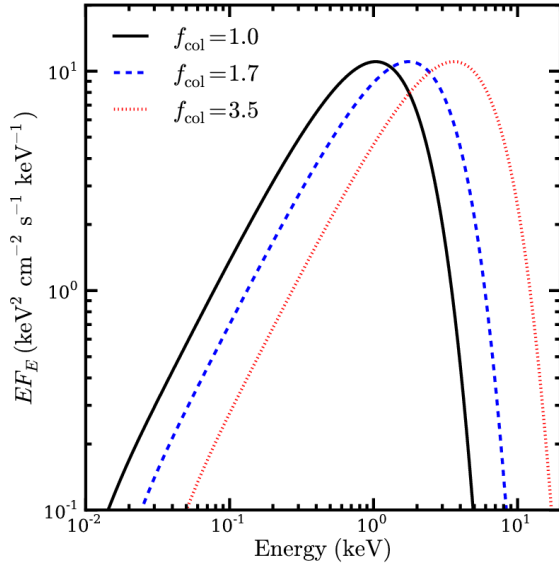


**Figure 3:** Spectrum — energy flux vs. photon energy — of an accretion disk from a BHXRBB with different levels of modification: none (*black solid line*), minor (*blue dashed line*), major (*red dotted line*).

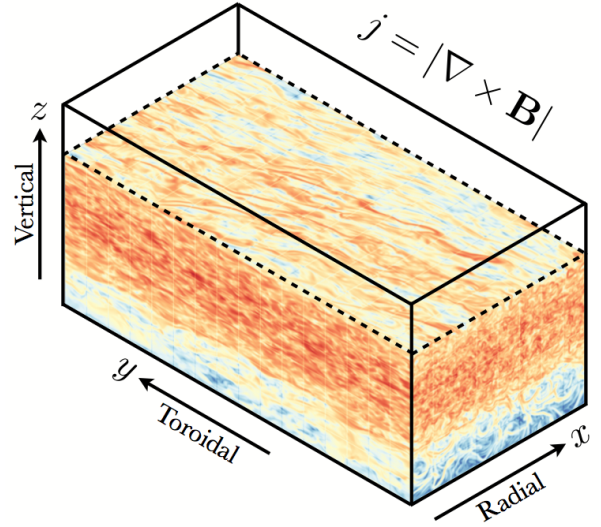


**Figure 4:** Snapshot from a simulation of a local patch of an accretion disk. Ribbon-like features in the rendering trace regions of swirling magnetic field, which is where energy gets released.

Often times, observers assume a razor thin disk; in other words, one in which the accretion disk atmosphere does not exist. As a result, they use the *effective temperature* or  $T_{\text{eff}}$  in calculations—this is what the disk emits. But because there is evidence that an atmosphere does exist in reality, the light is subject to the effects of absorption, Compton scattering, and coronal dissipation. Thus, the light tends to be shifted to higher or “harder” energies. Nonetheless, this light that is measured still has the shape of a blackbody, so astronomers end up fitting the data to whatever temperature fits the shape – this is called the *color temperature*,  $T_{\text{col}}$ . During this fitting routine, however, the amplitude of the blackbody is not considered, so there must be some sort of conversion factor to relate the two temperatures. This is the *color correction factor*,

$f_{\text{col}}$  and the relationship between  $T_{\text{eff}}$  and  $T_{\text{col}}$  is characterized by

$$T_{\text{col}} = f_{\text{col}} T_{\text{eff}}.$$

Accretion disks are ubiquitous in astrophysics, playing key roles in planet formation, star formation, black hole phenomena, and galactic processes. Accretion is the most efficient means by which to convert energy into radiation, with this efficiency exceeding that of nuclear fusion tenfold. Therefore, understanding accretion in astrophysics is akin to understanding the most energetic phenomena in the Universe, justifying why accretion disks remain an exciting topic of active research.

## 2 Modeling the Accretion Disk Spectrum

The predicted spectrum from an accretion disk around a black hole was first calculated by Nikolay Shakura and Rashid Sunyaev in 1973 [18] with their derivation of the disk equations. Many of the concepts surrounding the accretion disk community had already been discussed, but Shakura and Sunyaev unified and brought mathematical equations to these ideas which seemed to model the physics that were seen. Most importantly, they obtained solutions for geometrically thin accretion disks, i.e., they have a scale height much less than the radius of the disk and the effective temperature profile of a disk goes as  $T(R) \propto R^{-3/4}$ ; more specifically,

$$T_{\text{eff}}(R) = \left\{ \frac{3GM\dot{M}}{8\pi R^3\sigma} \left[ 1 - \left( \frac{R_{\text{in}}}{R} \right)^{1/2} \right] \right\}^{1/4} \quad (1)$$

where  $G$  is the gravitational constant,  $M$  is the mass of the black hole,  $\dot{M}$  is the mass accretion rate,  $\sigma$  is the Stefan-Boltzmann constant, and  $R_{\text{in}}$  is the inner radius of the accretion disk (which for our purposes, is located at the innermost stable circular orbit ( $R_{\text{ISCO}}$ ) around the black hole<sup>3</sup>).

Kazuhisa Mitsuda [12], Kazuo Makishima [9] and their collaborators were among the first astrophysicists (1984 and 1986, respectively) to fit actual data using this model, proving its use and application to physical quantities rather than just being a theory of accretion disk mechanics. Neglecting the vertical structure (i.e., temperature, ionization state) of the disk and assuming the disk is optically thick, Mitsuda coined this the *Multicolor Disk Model* (MCD) where the only two free parameters are a characteristic temperature and a normalization factor solely dependent on the inner radius, disk inclination, and distance to the disk.

---

<sup>3</sup>Details of this assumption will be discussed in the Analysis & Results section.

With these assumptions, each annulus of the disk would radiate roughly as a blackbody with the temperature distribution in equation 1. Thus, the observed spectral flux from the entire disk would be:

$$F_E = N \frac{4\pi E^3}{h^3 c^2} \int_1^\infty \frac{r}{e^{E/kT_{\text{eff}}(r)} - 1} dr$$

where

$$N = \left( \frac{R_{\text{in}}}{D} \right)^2 \cos(i),$$

$E$  is energy,  $h$  is Planck's constant,  $c$  is the speed of light,  $k$  is the Boltzmann constant,  $D$  is distance to the system,  $i$  is the inclination of the disk, and  $r = \frac{R}{R_{\text{in}}}$ .

Since these early considerations of the spectrum emitted by a BHXR accretion disk, various works have investigated how the theoretical spectrum becomes modified in the presence of additional physics. In Toshiya Shimura and Fumio Takahara's 1995 paper [19], the disk equations began to evolve to include the color correction factor,  $f_{\text{col}}$ , since astronomers observe the color temperature instead of the effective temperature. By solving for the vertical structure as well as the radiative transfer simultaneously throughout the disk, they found that the inclusion of this spectral hardening factor is necessary to describe the shift in the spectrum that is observed—shifts caused by scattering, absorptive and emissive opacities, and Comptonization. For accretion rates nearing the Eddington limit, they report that  $f_{\text{col}} = 1.7 - 2.0$  is an appropriate range which will fit the spectrum observed from the BHXR. They also find that  $f_{\text{col}}$  is independent on radius or on the mass accretion rate. Thus, the new total flux from the disk is characterized as:

$$F_E = A \frac{4\pi E^3}{h^3 c^2} \int_1^\infty \frac{r}{e^{E/kf_{\text{col}}T_{\text{eff}}(r)} - 1} dr \quad (2)$$

where

$$A = \frac{1}{f_{\text{col}}^4} \left( \frac{R_{\text{in}}}{D} \right)^2 \cos(i).$$

This is the basis for the diluted blackbody or *Modified Multi-Color Disk Blackbody Model*: “Modified” originating from the inclusion of  $f_{\text{col}}$  and “multi-color” from the integration of light over all energies. Unlike the disk model put forward by Shakura and Sunyaev, the addition of  $f_{\text{col}}$  is entirely phenomenological. Its inclusion seems to work—it models what we see, but what observers measure in these systems is much more complicated than the output which these equations give. Yet, these estimates are sufficient for modeling the majority of accretion disk spectra from observed BHXBs.



Examples of processes operating in a real BHXRB accretion disk that contribute to altering the more simplistic spectrum include: (1) high-energy electrons scattering low-energy photons up to higher energies [14], (2) absorption and emission of radiation from atomic processes [5], and (3) relativistic effects due to the extreme space-time in the close vicinity of the black hole [15]. The bottom line is that the overall effect of these complicated physical processes is that the predicted accretion disk spectrum experiences a relatively minor, but important, shift toward higher energies, as shown by the *blue dashed line* in Figure 3. Fortunately, a single parameter,  $f_{\text{col}}$ , is usually adequate to capture the global effect of the aforementioned physics on the actual observed accretion disk spectra from BHXRBs.

Moreover, the ultimate objectives of this research are: (1) *To use theoretical techniques to quantify how redistributing the energy contained in the accreting gas modifies the accretion disk spectrum, and (2) to determine whether the degree of spectral modification can be constrained with current X-ray observations of accretion disk spectra.* The work that follows in this thesis will show that theoretical data of a disk spectrum can be fitted to a model using only two parameters— $N$  and the maximum temperature of the disk—placing bounds on these values by limiting them to only physically-meaningful ranges. I attempted to fit the data to a model with an additional parameter,  $f_{\text{col}}$ , but parameter degeneracies did not allow the Least Squares fitting algorithm to find optimal values. To ensure that the two-parameter model was working, I also computed a grid of  $\chi^2$  values for a particular  $f_{\text{col}}$  to test goodness of fit, exploring every possible combination of  $N$  and  $T_{\text{max}}$  in their respective ranges to find the best fit values.

### 3 Analysis & Results

#### 3.1 Modified Multi-Color Disk Blackbody Model

To better understand how the MCD model depends on its numerous parameters, it is helpful to see how each of them changes the disk spectrum. Below, I explore each of the parameters present in equation 2, explaining their influence on the emitted disk spectrum. Each of the sections has a corresponding figure for a visual comparison.

**Inclination** is one of the many parameters present in the disk spectrum equations. Although a disk does not have an intrinsic orientation on the sky, how it is positioned relative to the observer changes the light that we can see. A disk with an inclination of  $0^\circ$  is called face-on and a disk with an inclination of  $90^\circ$  is edge-on. It is certainly easy to imagine that if the disk is face-on, the telescope receives more light, i.e.,

there is a higher emitting area. The physical tilt of the disk is independent of energy and thus, there is no horizontal shift in the spectrum (see Figure 5), only a change in amplitude.

The **outer radius**, while often not specified beyond a reasonable number, also has an effect on the spectrum that we see (reference Figure 6). In comparison to a small disk, a larger disk has a greater number of annuli far away from the black hole; thus, it has lower temperatures in these annuli and as a result, lower energies. However, the spectrum is a summation of individual blackbody spectra over all annuli so a bigger disk would give a higher total flux since there are more annuli contributing to the disk spectrum. In addition, the annuli closer to the black hole would be the same regardless of disk size, so we would expect an identical disk spectrum in the higher energy region. Finally, the outer radius also sets the low-energy turnover point: a smaller disk produces a turnover at a higher energy. In practice, this is often not considered since the low-energy turnover due to  $R_{\text{out}}$  is outside the observable band.

**Mass** is one of the most important parameters in the disk spectrum equations because it has such a noticeable effect on what is observed, as seen in Figure 7. Consider the following scaling of equation 1.  $T_{\text{eff}} \propto \frac{M^{1/4}}{R_{\text{in}}^{3/4}}$ . With the assumption that  $R_{\text{in}} \sim R_{\text{ISCO}} \propto \frac{GM}{c^2}$ , this implies that  $T_{\text{eff}} \propto \frac{M^{1/4}}{M^{3/4}} = M^{-1/2} = \frac{1}{M^{1/2}}$ . From this back-of-the-envelope comparison, it is easy to see that increasing mass will decrease the temperature of the disk. Hence, supermassive black hole accretion disks are cooler than stellar mass black hole accretion disks and emit predominantly in the Ultraviolet (UV) rather than the X-ray band.

The parameter of black hole **spin**, usually denoted as  $a$ , is not an explicit variable in the disk equations. However, spin is often used to calculate estimates of  $R_{\text{ISCO}}$  [2], which is a parameter used in the model. The spin of a black hole and its inner radius have an inverse monotonic relationship: a spin of -1 merits an  $R_{\text{ISCO}} = 9R_g$ , or 9 gravitational radii, a spin of 0 gives  $R_{\text{ISCO}} = 6R_g$ , and a spin of 1 gives  $R_{\text{ISCO}} = 1R_g$ , where  $R_g = \frac{GM}{c^2}$ . As a result, the temperature increases and the spectrum hardens. The disk spectrum will reach a maximum flux at a higher energy so it becomes “harder” (see Figure 8). However, the slope of the power law section of the spectrum will remain unchanged despite its change in extent.

**Mass accretion rate**, or how fast the material is falling onto the black hole, changes the overall temperature of the disk. A higher  $\dot{M}$  will be hotter than a system with a lower accretion rate; thus the disk will emit at slightly higher energies and will have a higher total flux (see Figure 9). One could easily reparametrize the disk equations to be a function of  $\dot{M}$  instead of temperature.

The **distance** to a BHXRB only has an effect on the amount of light that reaches the observer. Because the total flux of the disk is  $\propto \frac{1}{D^2}$ , if a system was twice as far away as another, but both had equal luminosity,

we would see 1/4 the amount of light from the farther system than the closer system. This explains how the flux of the disk is smaller as a function of distance, as illustrated by Figure 10.

Because there are so many parameters which must be included in the disk model, it is important to know how to distinguish one spectrum from another so that identifying properties (i.e. mass, spin, etc.) can be solved for. Nevertheless, there is no way to separate some of the parameters from the others. Take, for example, the spin and mass of the black hole. In each case, a higher spin and a higher mass shift the spectrum to the right, towards higher or “harder” energies. There is no way to know whether the shift in an observed spectrum originates from the spin or the mass therefore creating problems in understanding the actual structure of the disk. In addition, there are frequent issues in trying to measure each of these parameters accurately. If the astronomer cannot sufficiently estimate these values, the output spectrum loses meaning since there is just too much unknown and uncertain information.

One of the subtleties of the MCD blackbody model is the assumption that the inner radius of the accretion disk is at  $R_{\text{ISCO}}$ . A standard assumption in the literature is exactly the one we have made here, but many of the spectral fitting packages used to fit data with the model assume a nonzero torque at the inner boundary. Because the radiation from various annuli does not exactly equal the change in gravitational binding energy as material moves inwards, the disk structure highly depends on the location and the boundary conditions at the inner radius. Much of the motivation for this model arises from the idea that the “gas viscous inspiral timescale is long relative to the free-fall timescale for gas at the  $[R_{\text{ISCO}}]$ ” [17]. For this reason, the gas inside the inner most stable circular orbit does not have time to radiate before plunging into the black hole. However, this is an active area of research since some have proposed that the magnetic fields within a disk act as a method of communication between the material and the rest of the accretion disk, allowing energy and angular momentum to be extracted from the gas [7]. Nevertheless, for the purpose of this research, it is acceptable to let the inner radius of the accretion disk be at the same location as the innermost stable circular orbit.

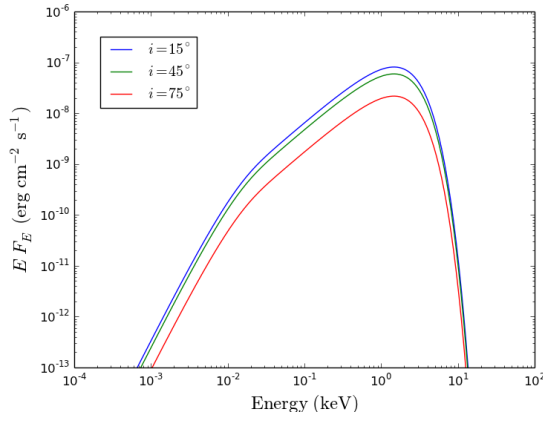


**Figure 5:** Accretion disk spectra with variations in inclination.

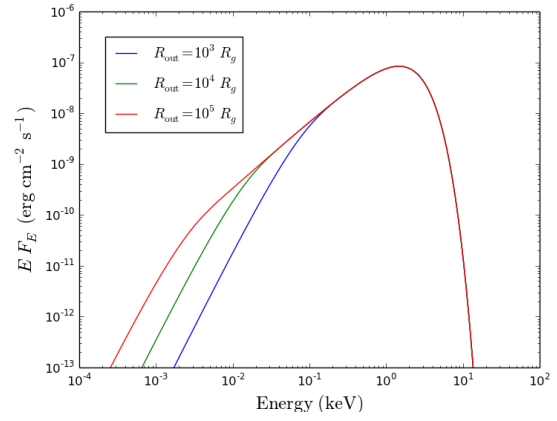


**Figure 6:** Accretion disk spectra with variations in outer radius.

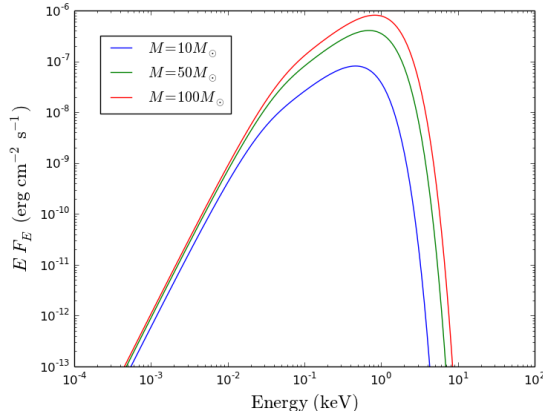


**Figure 7:** Accretion disk spectra with variations in mass.

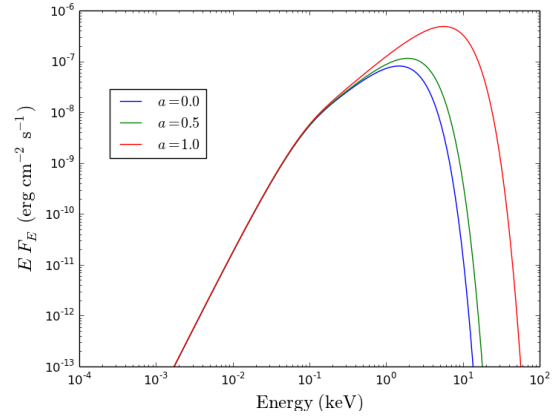


**Figure 8:** Accretion disk spectra with variations in black hole spin.

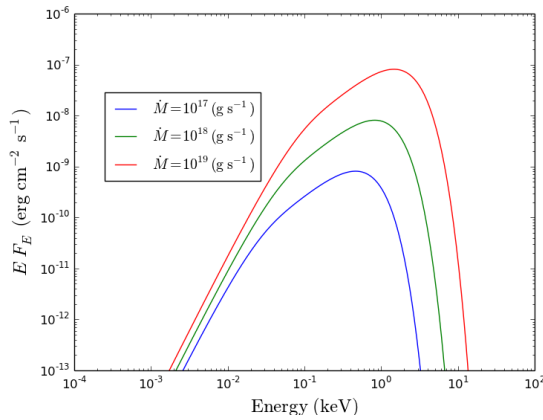


**Figure 9:** Accretion disk spectra with variations in mass accretion rate.

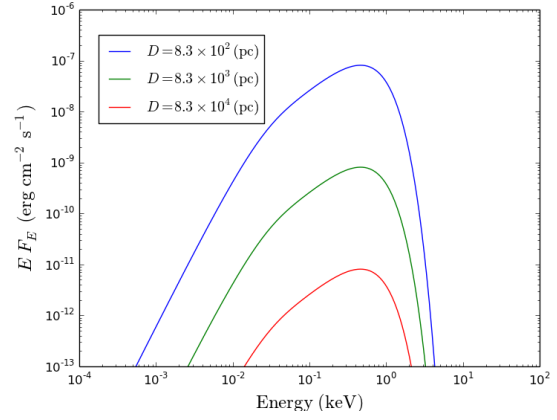


**Figure 10:** Accretion disk spectra with variations in distance.

While the zero-torque boundary condition imposed on  $T_{\text{eff}}$  is useful for modeling, there are various parameters which are unknown in practice, such as mass, the mass accretion rate, and the inner radius. Reparametrizing this in terms of known quantities like the maximum temperature reached in the disk is a more accessible way of using this equation.

Let  $r = \frac{R}{R_{\text{in}}}$ , a dimensionless radius. Then,

$$T_{\text{eff}}(r) = \left[ \frac{3GM\dot{M}}{8\pi R_{\text{in}}^3 \sigma} \right]^{1/4} r^{-3/4} (1 - r^{-1/2})^{1/4}. \quad (3)$$

While the temperature

$$T_* = \left[ \frac{3GM\dot{M}}{8\pi R_{\text{in}}^3 \sigma} \right]^{1/4} \quad (4)$$

is somewhat meaningless because it is not a physical temperature that is found anywhere in the accretion disk, we can substitute 4 into equation 3 and rewrite it as

$$T_{\text{eff}}(r) = T_* r^{-3/4} (1 - r^{-1/2})^{1/4}. \quad (5)$$

However, the maximum temperature of the disk occurs at  $r = \frac{49}{36}$  [6] and because it is meaningful, we can reparametrize in terms of  $T_{\text{max}}$ . Plugging in  $r = \frac{49}{36}$ ,

$$\begin{aligned} T_{\text{max, eff}} &= T_{\text{eff}}\left(r = \frac{49}{36}\right) \\ &= T_* \left(\frac{49}{36}\right)^{-3/4} \left[1 - \left(\frac{49}{36}\right)^{-1/2}\right]^{1/4} \\ &= T_* \left(\frac{49}{36}\right)^{-3/4} \left(\frac{1}{7}\right)^{1/4} \\ &\approx 0.488 T_*. \end{aligned} \quad (6)$$

This implies that

$$\begin{aligned} T_* &= T_{\text{max, eff}} \left(\frac{49}{36}\right)^{3/4} 7^{1/4} \\ &\approx 2.05 T_{\text{max, eff}}. \end{aligned} \quad (7)$$

Finally, substituting 7 into 5,

$$\begin{aligned} T_{\text{eff}}(r) &= T_{\text{max, eff}} \left( \frac{49}{36} \right)^{3/4} 7^{1/4} r^{-3/4} (1 - r^{-1/2})^{1/4} \\ &= T_{\text{max, eff}} 6^{-3/2} 7^{7/4} r^{-3/4} (1 - r^{-1/2})^{1/4} \end{aligned} \quad (8)$$

and we have a radial temperature distribution which depends on the astronomer only knowing *one* parameter: the maximum temperature of the disk. In order to compute the total disk flux as exhibited by equation 2, we must also know the normalization, which is given by  $A$ . However, since  $f_{\text{col}}$  is one of the parameters that I will attempt to fit, the normalization factor will be defined as

$$N = \left( \frac{R_{\text{in}}}{D} \right)^2 \cos(i).$$

### 3.2 Analysis Tool: Fitting Algorithm

In order to investigate how the redistribution of energy available in the accreting gas affects the observed accretion disk spectrum from a BHXRB, I attempted to fit BHXRB data to the model using only three free parameters: (1) a normalization which scales the flux, found as  $N = (\frac{R_{\text{in}}}{D})^2 \cos(i)$ , the maximum temperature  $T_{\text{max}}$ , and the color correction factor  $f_{\text{col}}$ . Much of the challenge when working with real data is that it is not nearly “good enough” to accurately fit it to a model to find out how the unknown parameters (in this case,  $N$ ,  $T_{\text{max}}$ , and  $f_{\text{col}}$ ) vary over BHXRB systems.

As a result, I created a program in Python which constructs a disk spectrum from any values of mass, mass accretion, etc., which I provide it with. In order to find  $R_{\text{ISCO}}$ , I used the equations from James Bardeen’s 1972 paper [2] which give the relation between spin and  $R_{\text{ISCO}}$ . Following this, I now had either calculated or given the program enough information to determine the temperature profile of the disk, equation 1. Then I was able to calculate the monochromatic (single color/energy) flux for each of the annuli in the disk by integrating over radius, using exactly equation 2. Computing this for every energy bin therefore allowed me to collect the total disk flux—a disk spectrum (examples shown in Figures 5-10)!

Consequently, I designed an analysis tool which accepts a disk spectrum as an input, adds a percentage of scatter ( $\sim 10\%$ ) so it is no longer perfect data, and attempts to fit the values of  $N$ ,  $T_{\text{max}}$ , and  $f_{\text{col}}$  to best model the data it is given. This time though, I did not calculate the effective temperature by equation 1 since the objective was to minimize the number of parameters that the observer is required to know. This

prompted the use of equation 8. In order to fit the data, I used the method of minimizing  $\chi^2$ , the well-known practice of testing a goodness of fit of an observed data set to a theoretical one:

$$\chi^2 = \sum \left[ \frac{\text{Observed} - \text{Theoretical Model}}{\sigma} \right]^2$$

where  $\sigma^2$  is the variance of the observation, or the estimates on error for the measurement. This program uses the Sequential Least Squares Programming method to minimize a function of several variables with a combination of parameter bounds and equality constraints. By placing bounds on  $N$ ,  $T_{\max}$ , and  $f_{\text{col}}$  and providing an “initial guess” of these unknowns, I was encouraging the algorithm to hone in on values which would give the best fit to the model. [19] [21].

### 3.3 Proof of Concept

Knowing that the  $\chi^2$  minimization method is working is merely comparing the output values of the fitting algorithm to the calculated values from the perfect disk spectrum which I gave the algorithm; in other words, I have the correct answer from the perfect disk spectrum I created and I am now making sure that this algorithm of only three parameters can accurately represent the same data constructed with six parameters.

However, complications with this algorithm arose when I tried to isolate  $f_{\text{col}}$  as a parameter to be fit in addition to the normalization factor and maximum temperature of the disk.  $N$  has the effect of shifting the disk spectrum’s amplitude as seen by Figures 5, 8, and 9; it has a higher amplitude overall with a higher normalization factor since it depends heavily on spin (which determines the inner radius), distance, and inclination.  $T_{\max}$  changes the spectrum in both the horizontal and vertical directions. Consider equation 1, which has a significant dependence on  $M$ ,  $\dot{M}$ , and spin. While it can be hard to imagine what effect synthesizing these parameters has on a disk spectrum, increasing each of these variables heightens the amplitude and shifts the graph to higher energies (refer to Figures 7, 8, and 9). Finally, it is clear from Figure 3 that a higher  $f_{\text{col}}$  shifts the spectrum toward harder energies. Because there is some overlap (i.e. degeneracy) in each of these variables in terms of their effects on the disk spectrum, the algorithm has a hard time finding a global minimum of  $\chi^2$ . There may have been multiple local minimums at which point the algorithm was uncertain of which combination of parameters to choose. In essence, the fitting algorithm could not find the mixture of  $N$ ,  $T_{\max}$ , and  $f_{\text{col}}$  that would best recreate the input disk spectrum data.

Despite this issue, the algorithm accurately fits the disk spectrum data for  $T_{\max}$  and  $N$ , while holding

$f_{\text{col}}$  constant at 1.0. Below, I have fit three different disk spectra (Figures 11, 13, 15), each with different values of spin and drawn the line of best fit (red) and the error bars every five data points (magenta). Each of these plots has an associated color contour plot which illustrates the expanse of  $\chi^2$  as a function of  $T_{\text{max}}$  and  $N$  when I compute  $\chi^2$  in a brute force way (Figures 12, 14, 16). Looking at these contour plots, the area of the darkest blue is where  $\chi^2$  is at a minimum. The two corresponding values of the normalization and maximum temperature are what my algorithm should find if it is fitting correctly since two different methods looking for a minimum chi-square should produce the same value. The reduced chi-squared statistic,  $\chi_v^2$ , is reported on the graph and is defined as a normalized  $\chi^2$  by the number of degrees of freedom,  $v$ . The number of degrees of freedom is given by the number of data points minus the number of parameters, where here the number of parameters is two, ( $T_{\text{max}}$  and  $N$ ). The values of the parameters used to generate the fake data set are as follows:  $M = 7.5M_{\odot}$ ,  $\dot{M} = 10^{19}$  g/s,  $i = 0^\circ$ ,  $D = 8.5$  kpc,  $f_{\text{col}} = 1.0$ , and  $R_{\text{out}} = 10^4 R_g$ .

In each of the plots, the printed numbers for  $N$  and  $T_{\text{max}}$  as determined by from the least squares fitting and brute force methods may be slightly different from each other. There could be two causes contributing to this effect: (1) When calculating the minimum  $\chi^2$  value for every combination of  $N$  and  $T_{\text{max}}$ , I am choosing a given resolution for the algorithm to decide on “how quickly” to step through the range of values. For instance, I could ask it to go from one to five in one step, five steps, 100 steps, etc. Each of these would give a slightly different answer: choosing smaller step sizes would give better resolution and the algorithm could focus in on a more precise combination of the parameters. (2) When I choose to optimally minimize  $\chi^2$  with least squares fitting, I can give the algorithm a tolerance level for when to stop tweaking its guesses on the parameter values. If I require a tolerance of one, for example, the algorithm would stop fitting the data when the  $\chi^2$  value no longer changes by one as it alters its guesses for  $N$  and  $T_{\text{max}}$ . A lower tolerance would require the algorithm to keep tweaking the guesses until it has met the required level. It is a combination of each of these two effects that is causing this minor discrepancy in the minimum  $\chi^2$  between the two methods, but for the purpose of ensuring the model works, the choices I have made will suffice.

Finally, I made one other assumption in the construction of these plots. Rather than integrate from 0.01–100 keV, a large range which gives me the entire spectrum and which I used to create the parameter plots (Figures 5–10), I chose to integrate from 0.1–25 keV which captures the range of energies which would typically be observed by X-ray telescopes, such as the Rossi X-ray Timing Explorer. This does, however, leave off the low-energy portion (Rayleigh-Jeans portion) of the spectrum which is determined by  $R_{\text{out}}$ . Should I have included the entire spectrum into the fitting algorithm,  $\chi^2$  would be further from a value



which indicates “a good fit” because the lower-energy turn-over caused by  $R_{\text{out}}$  proved difficult to fit.

Spin:  $a = 0.0$

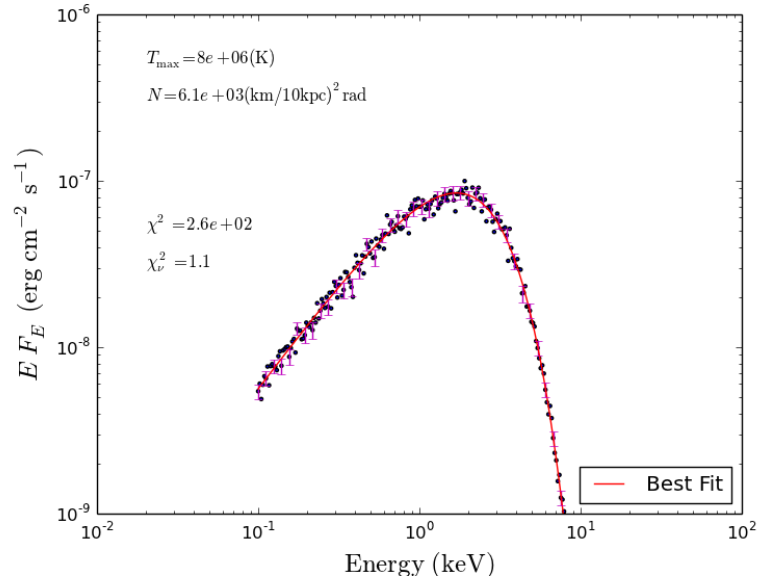


**Figure 11:** Accretion disk spectrum with 10% scatter, spin = 0.0 and its line of best fit and errors.

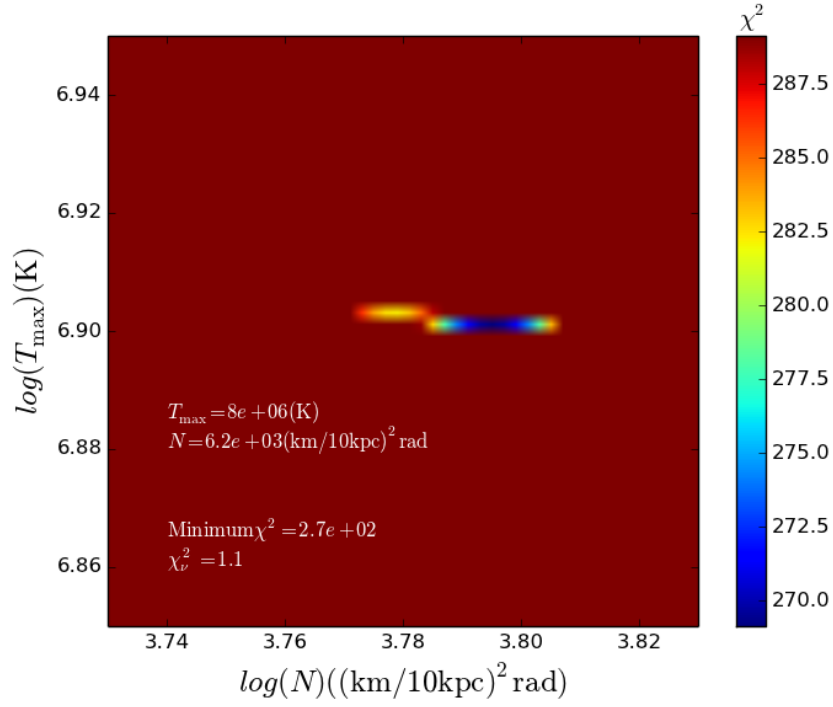


**Figure 12:**  $\chi^2$  contours of an accretion disk spectrum with 10 % scatter and spin = 0.0.

Spin:  $a = 0.5$

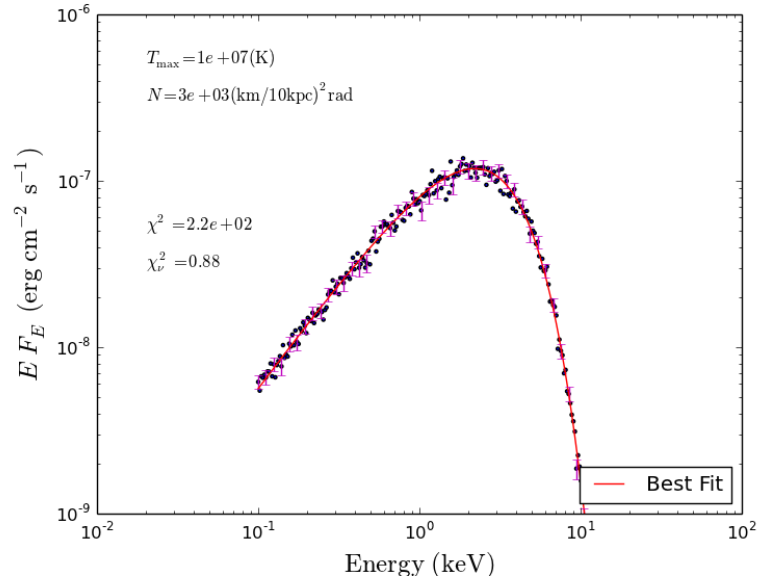


**Figure 13:** Accretion disk spectrum with 10% scatter, spin = 0.5 and its line of best fit and errors.

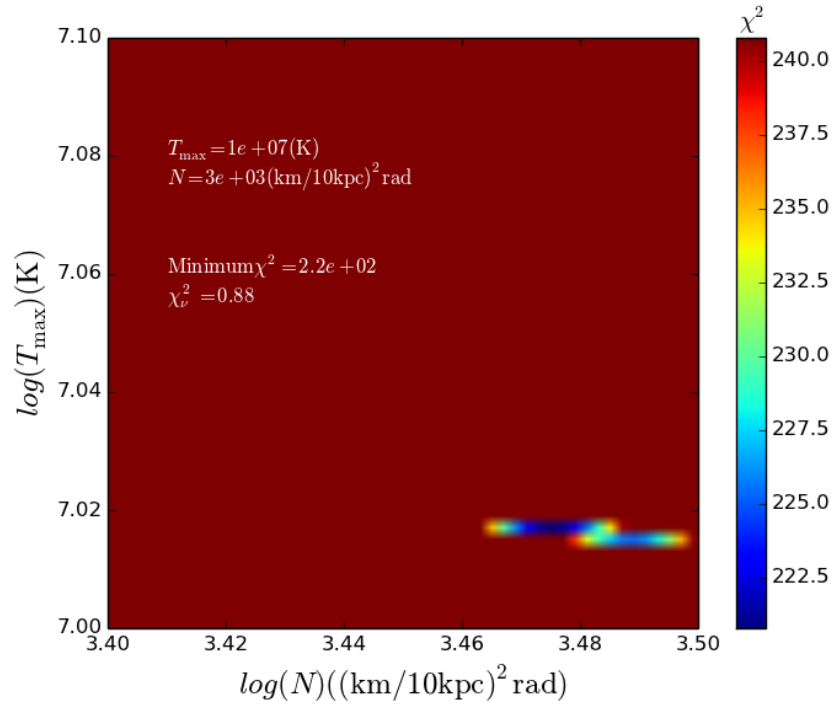


**Figure 14:**  $\chi^2$  contours of an accretion disk spectrum with 10 % scatter and spin = 0.5.

Spin:  $a = 1.0$

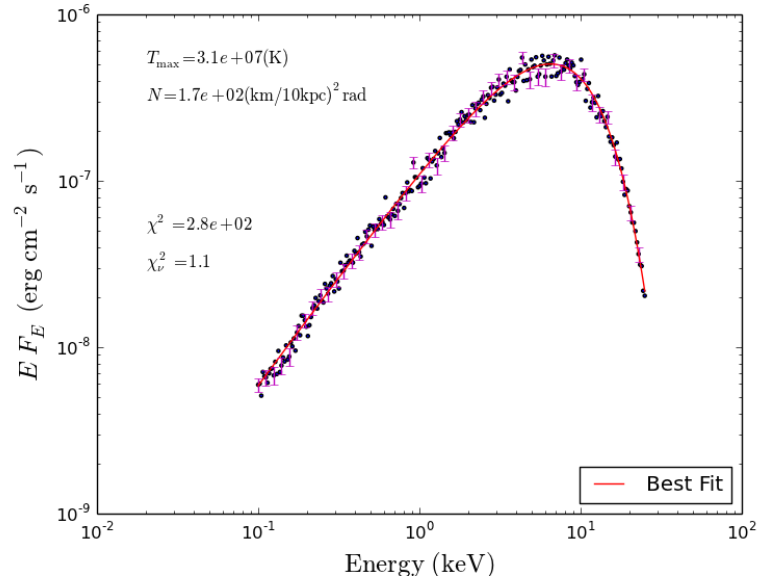


**Figure 15:** Accretion disk spectrum with 10% scatter, spin = 1.0 and its line of best fit and errors.

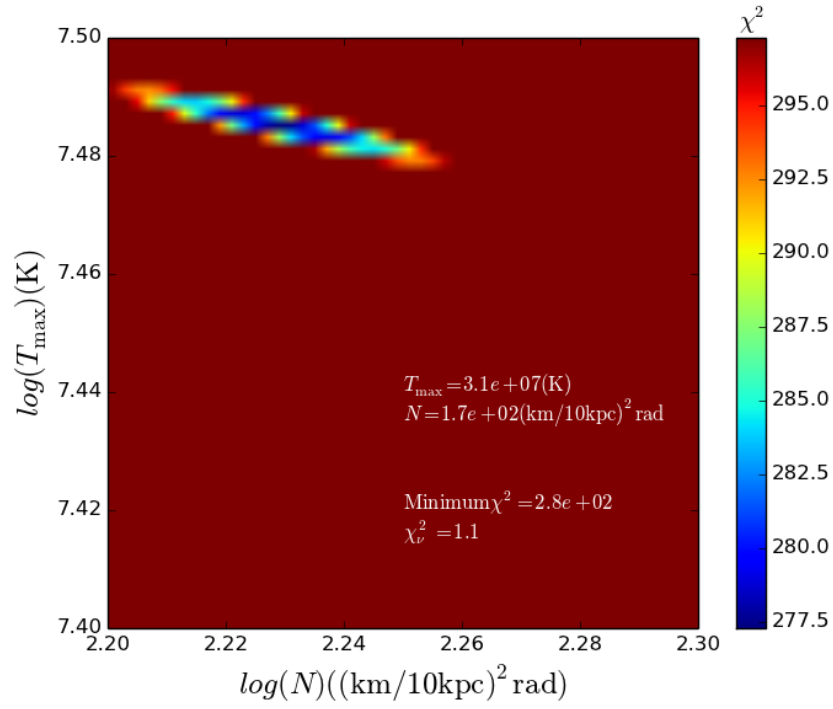


**Figure 16:**  $\chi^2$  contours of an accretion disk spectrum with 10 % scatter and spin = 1.0.

Below is a table summarizing the values computed for  $N$ ,  $T_{\max}$ , and  $\chi_v^2$ :

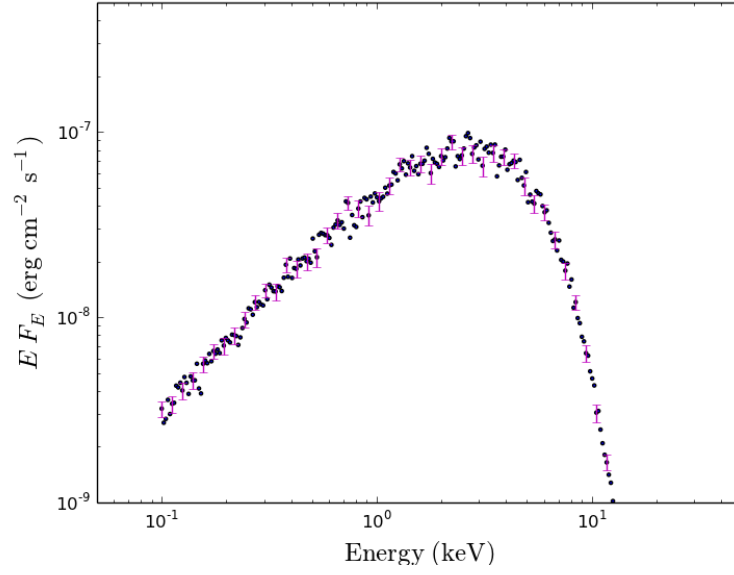
$a$	Actual $T_{\max}$	Actual $N$	$T_{\max, \text{LS}}$	$N_{\text{LS}}$	$\chi_{\text{LS}}^2$	$T_{\max, \text{BF}}$	$N_{\text{BF}}$	$\chi_{\text{BF}}^2$
0.0	6.901	3.786	6.902	3.789	265	6.901	3.795	269
0.5	7.016	3.482	7.016	3.481	218	7.016	3.476	221
1.0	7.486	2.229	7.486	2.229	277	7.486	2.229	277

Table 1: Summary of fitting results from two different methods of  $\chi^2$  minimization: least squares (LS) and a brute force grid (BF) for three different black hole spin values. The reported  $T_{\max}$  and  $N$  are their respective logarithms of the computed values and have their standard units of Kelvin and  $(\text{km}/10 \text{ kpc})^2$ .

### 3.4 The Difficulty of Using $f_{\text{col}}$ as a Third Parameter

As discussed in the previous subsection, the parameter degeneracies among  $N$ ,  $T_{\max}$ , and  $f_{\text{col}}$  proved too much for the algorithm to accurately fit an input disk spectrum. In the examples created above, I kept  $f_{\text{col}} = 1.0$ , a value which has no effect on the accretion disk model. In order to demonstrate the difficulty of using a third parameter, I created an input disk spectrum with a  $f_{\text{col}} = 1.6$  and  $a = 0.0$ , a standard value chosen in the literature. I then varied the disk model by hand, forcing it to select  $f_{\text{col}}$  as 1.4, 1.6, and 1.8 in order to change the relation of the data to the model and see how the values of the flux normalization,  $N$ , and maximum temperature vary with different selections of the color correction factor. Shown below are plots of the  $\chi^2$  contour, much like the ones before with varying spin. The true value of  $T_{\max} = 6.902 \text{ (K)}$  and the true value of  $N = 3.786(\text{km}/10 \text{ kpc})^2$  scaled logarithmically.

The below contour plots illustrate that even with just a 0.2 variation of  $f_{\text{col}}$  in the disk model from the data's actual value, 1.6, there is a large range of combinations of  $N$  and  $T_{\max}$  which give acceptable values of a “minimum”  $\chi^2$  (as indicated by the blue regions). When the model is given the absolute correct value of  $f_{\text{col}}$  (reference Figure 19), there are many values of  $N$  and  $T_{\max}$  which would minimize  $\chi^2$  according to the brute force method, suggesting the least squares fitting algorithm would have a difficult time choosing one combination over another. It is important to note that the axis ranges are not the same for each variation of  $f_{\text{col}}$ , done for the purpose of making clear where the minimum  $\chi^2$  occurs. Because of these complexities, incorporating  $f_{\text{col}}$  into the disk model as an additional parameter to be fit is currently a work in progress.



**Figure 17:** A visualization of the accretion disk spectrum used to vary  $f_{\text{col}}$  in the model. Here,  $a = 0.0$  and  $f_{\text{col}} = 1.6$ .

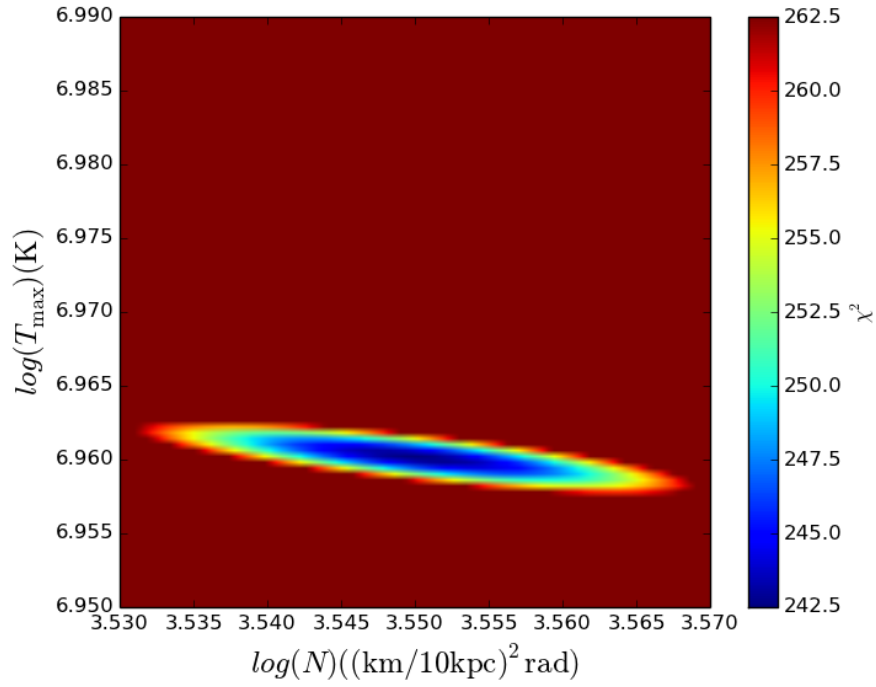


**Figure 18:**  $\chi^2$  contour plot with the model accepting  $f_{\text{col}} = 1.4$ .

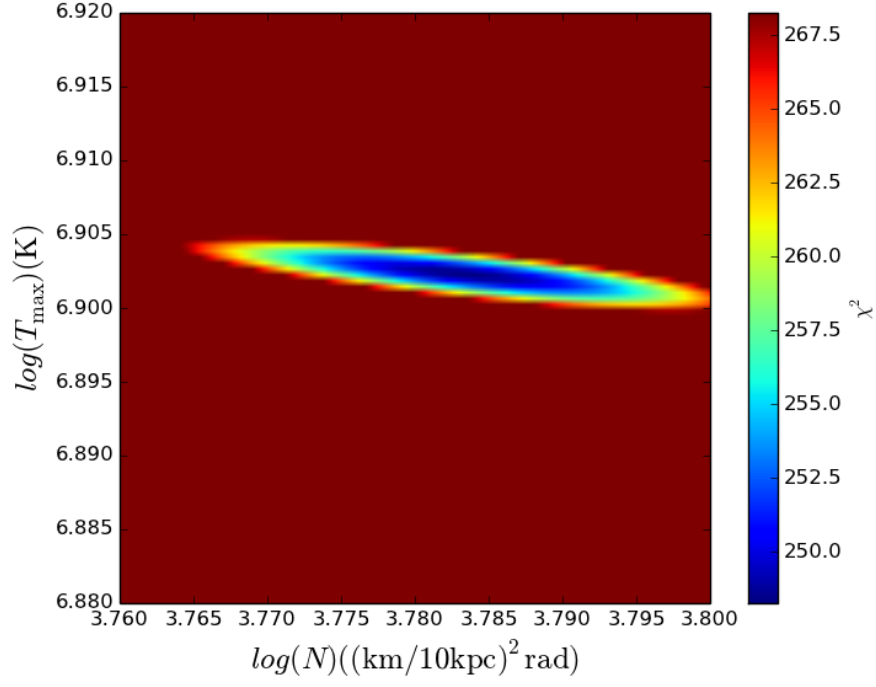


**Figure 19:**  $\chi^2$  contour plot with the model accepting  $f_{\text{col}} = 1.6$ .

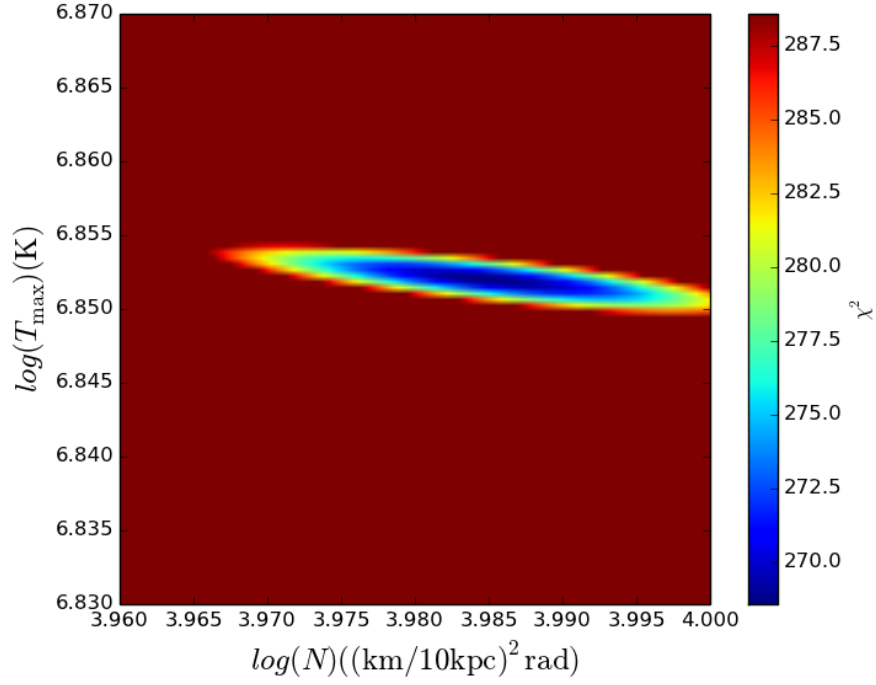


**Figure 20:**  $\chi^2$  contour plot with the model accepting  $f_{\text{col}} = 1.8$ .

## 4 Discussion

### 4.1 Future Research

The ultimate motivation for this research is continuing the findings of contributors before me. Roland Svensson and Andrzej Zdziarski offered a simple parametrization for redistributing some fraction,  $f$ , of the accretion power into the corona and recycled as heat or put into accelerating particles rather than being released as radiation [21]. They argue that magnetic buoyancy lifts the energy into the upper atmospheres of the disks. An equilibrium state in which the gas is partially supported against gravity by a toroidal magnetic field is unstable as field lines deform. Much like the Sun’s magnetic field carries material to the corona, the accretion disk magnetic fields carry the accretion energy to the atmosphere where magnetic reconnection dissipates it. In turn, this heats the gas and alters the vertical structure of the disk in an extremely complicated way.

Because  $f_{\text{col}}$  characterizes the shift in light observed due to this upper atmosphere, it is important to know whether the amount of energy that is carried into the corona has a significant effect on  $f_{\text{col}}$ . It is easy to imagine that the color correction factor is not a constant value, but may be a function of  $f$ , this amount of energy recycled in the atmospheres of the disk. Andrea Merloni is one of the first researchers to see if there is a relation between  $f_{\text{col}}$  and  $f$  [10]. In his 2000 paper, he suggests that the correlation is more important than is currently considered now. Although his models break down as  $f$  approaches 0.8 (80% of the energy is dumped into the corona), the range of  $f_{\text{col}}$  which accurately models BHXRBs is of higher values than what is typically used by observers. Shane Davis and his collaborators encourage Merloni’s findings in their 2005 paper concluding that “adopting a vertical dissipation profile... produces a large change in the disk structure... consistent with a  $\sim 10\%$  increase in the best fit  $f_{\text{col}}$ ” and that increasing the fractional dissipation would produce much larger changes. I was originally hoping to fit a three parameter disk model by way of Least Squares fitting, however, due to the parameter degeneracies, I was only able to fit a two parameter model. By employing Markov Chain Monte Carlo methods (MCMC), I am hoping to successfully fit the three parameter disk model to mock data, a set of disk spectra with different choices of  $f$ , constructed in a similar way that Merloni uses. I will fit these spectra and determine the relation between  $f_{\text{col}}$  and  $f$  by providing observers with a look-up table of which color correction factor is appropriate to use for their specific BHXRB system, given some knowledge of  $f$ . This method will allow me to fully explore the parameter space without the issue of parameter degeneracies and has been illustrated to work by Dipankar



Maitra and his collaborators in their 2014 paper, in which they analyzed 26 accretion disk spectra [8].

## 4.2 The Bigger Picture

Although the purpose of this research could simply come to understanding fundamental physics, much of the field is heading towards answering the question: *What is the ultimate fate of the accretion power in the disk and how does the disk spectrum we observe depend on this?* Knowing the answer to this question has consequences for many topics in astronomy. For instance, models for galaxy formation depend heavily on the spin of a black hole [22]. Because  $f_{\text{col}}$  and spin are degenerate parameters, measuring  $f_{\text{col}}$  is a way to measure the spin, which researchers must be confident in in order to theorize about galaxy formation. Only a handful of papers have successfully measured the spin of black holes at extremely high redshifts so increasing the certainty in the measurements of spin is essential to make strides in this area of research. Another area where this work is applicable is in the processes behind jets spewing from various astronomical objects. Some astronomers believe that somehow the system taps into the spin energy in order to pump the jet [4]. These are only two applications in the broader astronomical research picture relevant to this specific research.

## 5 Summary & Conclusion

Because the physical processes which occur in BHXRB accretion disks are so complex, modeling them is far from easy. The combined effect of scattering, absorption and emission, as well as relativistic effects translate into a hardening of the disk spectrum, characterized by the sole parameter of the color correction factor,  $f_{\text{col}}$ . Because of strong parameter degeneracies among the normalization, the maximum temperature of the accretion disk, and  $f_{\text{col}}$ , only a two parameter least squares fitting algorithm was successful—one which fit values for  $N$  and  $T_{\text{max}}$ . In order to ensure the correctness of this algorithm, I employed a second method of a brute force grid, which calculated  $\chi^2$  for all combinations of  $N$  and  $T_{\text{max}}$  within a physically-meaningful range. However, in order to find the relation between  $f_{\text{col}}$  and  $f$ , I will employ the use of MCMC in the future to successfully fit disk spectra to a three parameter model.

## References

- [1] Balbus, S. A., Hawley, J. F. et al. 1991, ApJ, 376, 214
- [2] Bardeen, J. M. et al. 1972, ApJ, 178, 347
- [3] Beloborodov, A. M. et al. 1999, ApJ, 510, 123
- [4] Blandford, R. D., Znajek, R.L. et al. 1977, MNRAS, 179, 433
- [5] Davis, S. W. et al. 2005, ApJ, 621, 372
- [6] Frank, J., King, A., Raine, D.. Accretion Power in Astrophysics. Third edition. Cambridge: Cambridge University Press, 2002. Print.
- [7] Krolik, J. H. et al. 1999, ApJ, 515, L73
- [8] Maitra, D. et al. 2014, ApJ, accepted for publication. arXiv ID: 1306.4365v2
- [9] Makishima, K. et al. 1986, ApJ, 308, 635
- [10] Merloni, A. et al. 2000, MNRAS, 313, 193
- [11] Miller, J. M. et al. 2009, ApJ, 707, L77
- [12] Mitsuda, K. et al. 1984, PASJ, 36, 741
- [13] Romani, R.W. et al. 1998, A&A, 333, 583
- [14] Ross, R. R. et al. 1978, ApJ, 219, 292
- [15] Ross, R. R. et al. 1996, MNRAS, 281, 637
- [16] Rosswog, S., Brüggen, M.. Introduction to High-Energy Astrophysics. Reprint edition. Cambridge: Cambridge University Press, 2011. Print.
- [17] Salvesen, G. et al. 2013, MNRAS, 421, 3510
- [18] Shakura, N. I. et al. 1973, A&A, 24, 337
- [19] Shimura, T. et al. 1995, ApJ, 445, 780
- [20] Simon, J. B. et al. 2012, MNRAS, 422, 2685
- [21] Svensson, R. et al. 1994, ApJ, 436, 599
- [22] Volonteri, M. et al. 2013, ApJ, 775, 94
- [23] Wijers. R. et al. 1996, ApJ, 463, 297
- [24] Zimmerman, E. R. et al. 2005, ApJ, 618, 832

$$\chi^2 = \sum_i \left[ \frac{y_{i,\text{theoretical}} - y_{i,\text{observed/data}}}{\sigma_i} \right]^2 \quad (9)$$

$$F_E = 2\pi N \int_1^\infty B_E(T_{\text{eff}}) r dr \quad (10)$$

$$\text{Brightness} = \frac{\text{Luminosity}}{4\pi \text{Distance}^2} \quad (11)$$